

Broadband Electromagnetic Radiation Absorber Based on Bifunctional Polymer–Magnetite Composite

O. AKSIMENTYEVA^{a,*}, S. MALYNYCH^{b,c},
R. FILIPSONOV^b AND R. GAMERNYK^d

^a*Department of Chemistry, Ivan Franko National University of Lviv,
8 Kyryla and Methodiya St., 79005 Lviv, Ukraine*

^b*Hetman Petro Sahaydachnyi Army Academy, 32 Heroes of Maidan St., 79026 Lviv, Ukraine*

^c*Lviv Polytechnic National University, 12 S. Bandery St., 79013 Lviv, Ukraine*

^d*Department of Physics, Ivan Franko National University of Lviv,
8 Kyryla and Methodiya St., 79005 Lviv, Ukraine*

Doi: [10.12693/APhysPolA.141.356](https://doi.org/10.12693/APhysPolA.141.356)

*e-mail: aksimen@ukr.net

We report on fabrication and studies of hybrid polymer-magnetite composite based on the thermoreactive epoxy resin filled with magnetite Fe₃O₄ particles and conductive conjugated polymer. The composite is capable of absorbing electromagnetic radiation in the broad spectral range, including microwaves and near-infrared. Dispersed magnetite Fe₃O₄ in the form of spherical particles with the diameter 1...2 μm provides effective scattering of infrared radiation, substantially reducing reflected infrared signal. It was also found that composite containing magnetic microparticles and particles of polyaniline doped with *p*-toluene sulfonic acid in a 1:1 ratio exhibits high hardness and provides exceptional anticorrosive properties when used as a coating on the surface of steel. Our findings may have wide potential applications, including effective electromagnetic radiation shielding and antiradar coatings.

topics: electromagnetic shielding, antiradar coating, magnetite, polyaniline

1. Introduction

Reducing the exposure of humans to the high-frequency alternating electromagnetic field is an important problem since more and more gadgets and electronic devices surround us permanently at work and leisure [1]. Despite its pervasive usefulness in all spheres of our life, electromagnetic radiation is one of the deplorable byproducts that can harm living organisms, as well as any kind of electronics. In the latter case, electromagnetic radiation may cause an unwanted disturbance that affects a circuit due to many superfluous radiated signals emitted from an external source carrying transient currents. In fact, two controversial problems arise when talking about the influence of electromagnetic radiation on electronic devices. Those are electromagnetic interference (EMI) that may interrupt, obstruct, or otherwise cause unacceptable degradation of system or equipment performance in terms of a partial or total loss of data, and electromagnetic compatibility (EMC), which is the ability of electrical equipment and systems to function properly in their electromagnetic environment [2]. Both factors must be attended, otherwise severe damage to communication systems and safety of operations of many devices

may occur. Effective microwave-absorbing materials are essential for security purposes in sensitive compartmented information facilities or SCIF (see, for instance, [3]). Thus, novel materials that absorb microwave radiation are of great interest in modern society.

Other practical applications, such as solar energy and military equipment, require surface coatings that effectively absorb not only microwave but also infrared (IR) radiation. Such coatings may substantially improve electromagnetic energy harvesting in thermal solar systems [4]. Those materials can also be used in stealth technologies that provide survivability of weapons [5–9]. Different materials and approaches, such as honeycomb structures [10], magnetic microwires [11], barium titanate perovskites [12], and NiZn ferrites [13], have been developed for that purpose to date. Recent progress in polymer materials, especially in conductive ones, opens wide possibilities to design radar absorbing materials and to utilize them for effective electromagnetic radiation (EMR) shielding. Polyaniline (PANI), the polymer with high electrical conductivity, easy preparation, excellent environmental stability, and availability of cheap monomers, is one of the promising candidates for broadband microwave

absorption applications [14, 15]. Ferromagnetic materials are known for their ability to absorb electromagnetic waves in near-infrared (NIR) and microwave ranges. It is natural to expect that nano- or micro-particulate ferrites will further facilitate the interaction between the composite and electromagnetic radiation in the desired manner due to the compatibility between the particles' size and the wavelength of EMR.

In the present work, we focus our studies on the fabrication of a composite coating possessing high absorption and low reflectivity in both microwave and NIR spectral ranges. The potential coating should also satisfy some other apparent conditions, such as low cost, easy fabrication and covering of the surface, adequate hardness, weatherproofness, and should protect the surface from the environment. Among other compounds, we suggest exploring epoxy resin as a matrix containing magnetite Fe_3O_4 particles along with conductive conjugated polymer — (PANI).

2. Materials and methods

Epoxy α -resin ED-20 with a hardener polyethylene polyamine (PEPA) was used as a binding material (matrix). To fabricate a composite material the epoxy matrix was filled with polyaniline and magnetite powder. Polyaniline was synthesized by oxidative polymerization of aniline solution under the action of an equimolar amount of the oxidizer ammonium persulfate. An aqueous solution of toluene-sulfonic acid (TSA) was used as a reactive surrounding and dopant, which improved the conductivity and plastic properties of the composite. Highly dispersed magnetite Fe_3O_4 was synthesized by alkaline hydrolysis of iron II and iron III salts with sodium oleate as a stabilizer. In order to provide better compatibility of the magnetic part with the epoxy matrix, the surface of magnetite nanoparticles was modified with a polystyrene shell [16]. Dispersed magnetite in the form of spherical particles (granules) with the size of about 1–2 μm was separated by magnetic decanting from the suspension. The resulting polymer composite was spilled onto a flat teflon substrate and peeled off the surface after final curing. Thus, free standing polymer composite film 0.2 mm thickness was obtained. Detailed synthesis procedure can be found elsewhere [17].

The filler samples of magnetite and PANI-TSA were characterized by X-ray and EDAX-analysis, Fourier transform infrared (FTIR) and Raman spectroscopy, and thermogravimetric techniques as described in [16–18]. Mechanical properties of the composites were studied by the Höppler consistometer [19, 20]. Microhardness or conic flow point was determined after indentation of the conical-end rod into the sample under the defined load and calculated from the expression

$$F_p = \frac{G}{A} = \frac{4G \times 10^4}{\pi h^2}, \quad (1)$$

where F_p is the microhardness [N/m^2] at the given load G [N], A is the area of a tip of the intended rod, and h is the penetration depth. Due to the fact that the values of F_p depend on the load G , we used the limit microhardness (F_∞) determined from the maxima on the microhardness vs. load curves. The error of the measurements does not exceed 5%. Composite samples for microhardness studies were prepared by pouring fluid composition into a teflon cylinder with a diameter of 0.5 cm and 0.8 cm depth. The composites were hardened at ambient temperature for 2 h and at $T = 50^\circ\text{C}$ for 1 h, after which they were removed from the mold and used for measurements.

Specific volume conductivity and temperature dependence of resistivity were measured with a 5 K/min rate. Powder sample was placed in quartz cylinder with dimensions $d = 5$ mm and $h = 2$ mm, between two nickel disc contacts equipped with built-in thermocouple under the pressure of 10 N/cm^2 . Microwave absorption was recorded with HP 8722C spectrum analyzer, CCD camera was used to record the NIR signal reflected from the surface of the composite.

The IR absorption spectra of the samples were acquired using an MDR-23 monochromator equipped with a halogen lamp as a light source. The samples were formed as films with an area of 1 cm^2 and a thickness of 0.2 mm by watering the resulting composition on the surface of teflon, curing at 50°C , and separation from the surface with the formation of “free” films.

3. Results and discussion

Typical images of Fe_3O_4 particles encapsulated in polystyrene shell and PANI/TSA composite with magnetic filler are presented in Fig. 1. Magnetite particles form spherical granules with an average size of 2 ± 0.5 μm , while the surface of the composite appears smooth and fairly uniform (Fig. 1b). X-ray diffraction peaks indicate the presence of cubic phase Fe_3O_4 particles with spinel structure and cell parameter $a = 8.3490(3)$ Å. X-ray diffraction studies performed on the composite reveal the prevailing amorphous structure of PANI/TSA with weak crystalline reflections. The average size of the crystallites is about 25–27 Å. The presence of TSA is confirmed by specific bands in FTIR spectra [16].

It was found that PANI/TSA samples possess high magnitude of conductivity $\sigma = 0.4$ – 0.5 S/m that exceeds the value of conductivity for a majority of acid doped PANI almost by the three orders of magnitude [21] and the value $\sigma = 0.28$ S/m for PANI doped with Y_2O_3 reported in [22]. The observed conductivity for PANI/magnetite composite confirms the validity of the composite for microwave attenuation/shielding. As the temperature of the sample increases, resistivity ρ of the composite decreases, which is typical for semiconductors.

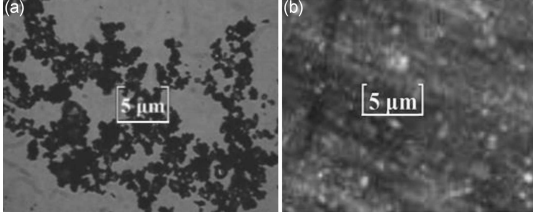


Fig. 1. Micrograph of magnetite Fe_3O_4 particles encapsulated into polystyrene shell (a); micrograph of the composite (5% magnetite +5% PANI/TSA powder) taken by “Olympus” optical microscope (b). A long-focus lens with a magnification of $50\times$ was used.

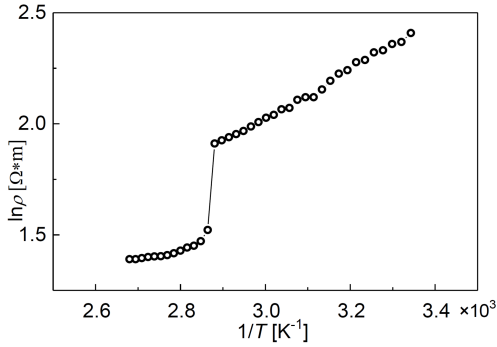


Fig. 2. Resistivity (natural logarithm) as a function of inverted temperature for PANI/TSA powder.

Temperature dependence of the resistivity can be fitted within 273–373 K temperature range by the expression $\rho = \rho_0 \exp(E_a/(2k_B T))$, where ρ is specific volume resistivity, E_a is the activation energy of charge transfer, k_B is Boltzmann constant, T is the absolute temperature, and ρ_0 is a constant. The activation energy of conductivity can be determined from the $\ln(\rho) = f(1/T)$ plot that yields $E_a = 0.17\text{--}0.19$ eV (Fig. 2). The abrupt change of resistance observed at the temperature $T = 370\text{--}373$ K corresponds to the desorption of chemisorbed on the sample’s surface moisture.

The composite exhibits excellent mechanical properties that make it perspective as a surface coating. To characterize the microhardness of a material, the limit between elastic and plastic deformation is often being used. In our case, the limit is designated as F_∞ and corresponds to the limit conic yield point of the material. Experimentally determined values of F_∞ illustrate that the microhardness of the composite depends on the amount of polymer filler and its chemical nature. Filling the epoxy matrix with PANI/TSA filler results in a substantial increase of F_∞ . The dependence of F_∞ on the amount of fillers is quite complex and for PANI/TSA dopant reaches the maximum at 5 wt%. Filling the matrix with magnetite also results in the increase of microhardness. The most prominent increase of the yield point up to 63×10^9 K/m²

TABLE I
Microhardness of the samples of different composition.

Samp. No.	Composition	Microhardness F_∞ ($\times 10^{-9}$) [N/m ²]
1	ED-20/PEPA	7.7
2	ED-20/PEPA+5% PANI-TSA	14.6
3	ED-20/PEPA+10% Fe_3O_4	31.2
4	ED-20/PEPA+15% Fe_3O_4	31.2
5	ED-20/PEPA+1% Fe_3O_4 +1% PANI	18.7
6	ED-20/PEPA+5% Fe_3O_4 +5% PANI	62.6
7	ED-20/PEPA+15% Fe_3O_4 +15% PANI	32.9*

*breaks after 5 N load

is observed when both PANI/TSA and magnetite fillers are introduced to the composite at the level of 5 wt% (see Table I). That indicates a synergetic effect when the influence of one component is enhanced by another one and proves the formation of a hybrid structure. At high fillers concentration, about 15 wt% microhardness of the composite decreases due to loosening effect and results in breaking of the sample. Thus, 5% magnetite with 5% PANI/TSA level of filling can be considered optimal since it provides the highest hardness.

Remarkably, this optimal composition (5% magnetite +5% PANI/TSA) also provides water resistance and excellent anticorrosive properties when used as a coating on the surface of steel. The relative water absorption by the composite coating after 30 days of exposure in a moist chamber with a humidity of 95% turned out to be 5–6 times less than that for unfilled epoxy composition. The electrochemical potential of the coated steel surface based on the developed thermosetting composition exhibits a significant anode shift (by 0.3–0.4 V), while the surface state of the coatings remained unchanged [23]. The obtained results confirmed the sufficient corrosion resistance of the coatings in comparison with the known analogues [24].

Studies of microwave absorption of the composite were performed with HP 8722C spectrum analyzer. The specimen of 0.2 mm thickness (sample number 6 in Table I) was placed across the waveguide normal to the direction of propagation of electromagnetic radiation. The composite film was cut to fit the internal cavity of the waveguide. Figure 3 depicts frequency dependence of RF radiation power absorption presented as $\log_{10}(P_I/P_T)$, where P_I and P_T are incident radiation power and transmitted radiation power respectively. The composite exhibit high attenuation of EMR in K band (18–26.5 GHz) and K_α band (26.5–40 GHz) on the level of -25 dB with a peak value of -47 dB at 23 GHz that makes the material perspective for electromagnetic radiation shielding and antiradar purposes. Shielding properties of similar composite materials based on epoxy resins with graphene nanoplates as filler in the microwave frequency range exhibit only 10 dB at 27 GHz [25].

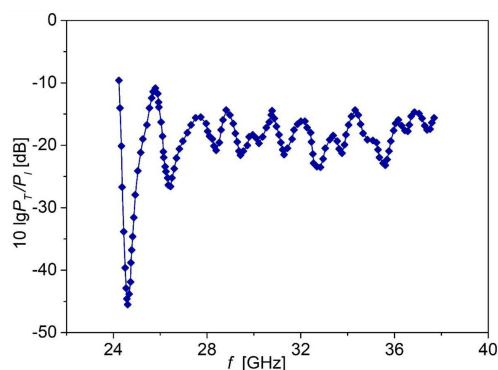


Fig. 3. RF radiation power absorption spectrum measured by HP 8722C spectrum analyzer for ED20/PEPA composites with 10% content of fillers (5% Fe_3O_4 + 5% PANI/TSA). Film thickness $0.2 \mu\text{m}$.

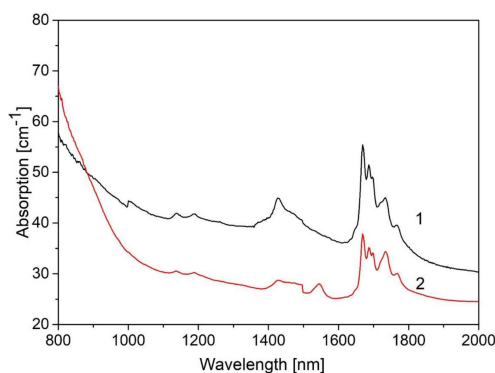


Fig. 4. IR absorption spectra of film samples of epoxy composition with different content of fillers: curve 1 — 5% magnetite + 5% PANI/TSA; curve 2 — 10% magnetite. Film thickness $0.2 \mu\text{m}$.

To study the absorption of the composites in the NIR range the film samples of different compositions were prepared. The IR absorption spectra of the samples were acquired using an MDR-23 monochromator equipped with a halogen lamp as a light source. The absorption spectra of the samples in NIR region with various filler abundance are shown in Fig. 4.

Our studies reveal that the composite containing magnetic microparticles and particles of polyaniline doped with TSA at a 1:1 ratio (Fig. 4, curve 1) exhibits the strongest IR absorption compared to a composite filled only with magnetite (Fig. 4, curve 2). At the same time, this composition exhibits high microhardness (see Table I, sample number 6).

Figure 5 illustrates exceptionally low reflectivity of the composite in NIR spectral range on the contrast to visual range. The samples were placed on the surface of black painted steel that serves as a background. A conventional digital camera was used to take a photograph of the sam-

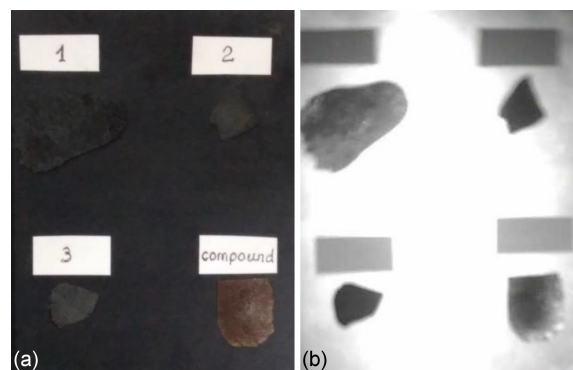


Fig. 5. Visual image of the samples of different composition on the black painted steel background (a); the same scene taken in NIR spectral range ($0.8\text{--}1 \mu\text{m}$) (b). Sample designation: compound — ED-20/PEPA matrix without fillers; curve 1 — epoxy compound with 1% Fe_3O_4 + 1% PANI/TSA; curve 2 — 15% Fe_3O_4 + 15% PANI/TSA; curve 3 — 5% Fe_3O_4 +5% PANI/TSA.

ples in visual range, while night-vision CCD was employed to acquire an IR image. LED operated at the wavelength 940 nm was used for illumination. It is seen clearly in Fig. 5b that the background shines brightly while the composite with fillers (5% Fe_3O_4 +5% PANI/TSA) and others remain dark. The reflection coefficient for that sample as measured by a spectrophotometer is about 2.5%, which converts to reflection loss -16 dB . Such coating may substantially improve EMR harvesting in solar thermal elements or be used as a protection against laser guided weapons.

4. Conclusion

We have synthesized composite material possessing high absorption of electromagnetic radiation in microwave and NIR spectral ranges. The composite comprises electrically conductive polyaniline polymer doped with TSA and magnetite microparticles stabilized by polystyrene shells. Such coating may find dual military and common purpose applications. The coating can be used for electromagnetic shielding, antiradar purpose, and as a highly absorbing IR material for light harvesting in solar thermal energy application.

References

- [1] D. Micheli, M. Marchetti, *Engineering* **4**, 928 (2012).
- [2] P. Mathur, S. Raman, *Journal of Electronic Materials* **49**, 2975 (2020).
- [3] National Counterintelligence and Security Center, *Technical Specifications for Construction and Management of Sensitive Compartmented Information Facilities*, 2020.

- [4] M. Lundha, T. Blomb, E. Wäckelgård, *Solar Energy* **84**, 124 (2010).
- [5] P. Thomas, L.V. Abdulhakim, N.K. Pushkaran, A.C. Karuvandi, *J. Carbon Res.* **6**, 72 (2020).
- [6] D. Micheli, R. Pastore, A. Vricella, M. Marchetti, in: *7th Int. Conf. on Recent Advances in Space Technologies (RAST), Istanbul*, IEEE, 2015.
- [7] C.G. Jayalakshmi, A. Inamdar, A. Anand, B. Kandasubramanian, *J. Appl. Polym. Sci.* **136**, 47241 (2019).
- [8] R.S. Biscaro, E.L. Nohara, G.G. Peixoto, R. Faez, M.C. Rezende, in: *Proc. 2003 SBMO/IEEE MTT-S Int. Microwave and Optoelectronics Conf. (IMOC 2003), Foz do Iguaçu (Brazil)*, IEEE, 2003, p. 355.
- [9] Y. Wang, T. Li, L. Zhao, Z. Hu, Y. Gu, *Energy Power Eng.* **3**, 580 (2011).
- [10] H. Luo, F. Chen, F. Wang, X. Wang, W. Dai, S. Hu, R. Gong, *AIP Adv.* **8**, 056635 (2018).
- [11] P. Marín, D. Cortina, A. Hernando, *IEEE Trans. Magn.* **44**, 3934 (2008).
- [12] Y. Akinay, F. Hayat, *J. Compos. Mater.* **53**, 593 (2019).
- [13] J. de Castro Dias, I.M. Martin, M.C. Rezende, *J. Aerosp. Technol. Manag.* **4**, 267 (2012).
- [14] R. Kumar, S. Joon, A. Pratap Singh, B.P. Singh, S.K. Dhawan, *Am. J. Polym. Sci.* **5**, 28 (2015).
- [15] L.C. Folgueras, M.A. Alves, M.C. Rezende, *J. Aerosp. Technol. Manag.* **2**, 63 (2010).
- [16] O.I. Aksimentyeva, V.P. Savchyn, V.P. Dyakonov, S. Piechota, Yu.Yu. Horbenko, I.Ye. Opainych, P.Yu. Demchenko, A. Popov, H. Szymczak, *Mol. Cryst. Liq. Cryst.* **590**, 35 (2014).
- [17] O.I. Aksimentyeva, I.B. Chepkov, R.V. Filipsonov, S.Z. Malynych, R.V. Gamernyk, G.V. Martyniuk, Yu.Yu. Horbenko, *Phys. Chem. Solid State* **21**, 764 (2020).
- [18] O.I. Aksimentyeva, I.Ye. Opainych, V.P. Dyakonov, S. Piechota, V.P. Zakordonskyi, P.Yu. Demchenko, H. Szymczak, *Phys. Chem. Solid State* **13**, 438 (2012).
- [19] N.M. Brailko, *Bull. UMSA* **19**, 150 (2019).
- [20] I. Opainych, O. Aksimentyeva, V. Dyakonov, S. Piechota, Ya. Ulanskii, P. Demchenko, A. Ukrainets, *Mater. Sci.* **48**, 95 (2012).
- [21] M. Trchová, J. Stejskal, *Pure Appl. Chem.* **83**, 1803 (2011).
- [22] M. Faisal, S. Khasim, *e-Polymers* **14**, 209 (2014).
- [23] O. Aksimentyeva, G. Martyniuk, Yu. Horbenko, S. Malynych, R. Filipsonov, *Phys. Chem. Mech. Mater.* **13**, 137 (2020).
- [24] L. Lv, W. Liu, *Mol. Cryst. Liq. Cryst.* **710**, 103 (2020).
- [25] N.I. Volynets, D.S. Bychenok, A.G. Liubimov et al., *Lett. JTP* **42**, 9 (2016) (in Russian).